Received: 29 July 2022 | Accepted: 1 February 2023

DOI: 10.1111/arcm.12853

ORIGINAL ARTICLE

Mortars in context: An integrated study of mortars and plasters from the so-called *Ginnasio* in Solunto (Sicily, Italy)

Beatrice Boese[1] | **Silvia Amicone**[1,2] | **Emma Cantisani**[3] | **Frerich Schön**[4] | **Christoph Berthold**[1]

[1]Competence Center Archaeometry—Baden-Wuerttemberg, Eberhard Karls University Tuebingen, Tübingen, Germany

[2]Institute of Archaeology, University College London, London, UK

[3]CNR Institute of Heritage Science (Florence Unit), Sesto Fiorentino (Florence), Italy

[4]SFB 1070 ResourceCultures, Eberhard Karls University Tuebingen, Tübingen, Germany

Correspondence

Beatrice Boese, Competence Center Archaeometry—Baden-Wuerttemberg, Eberhard Karls University Tuebingen, Wilhelmstraße 56, D-72074. Tübingen, Germany.
Email: beatrice.boese@uni-tuebingen.de

Abstract

This paper presents a multipronged scientific study of mortars and plasters of the so-called *Ginnasio* in the Hellenistic–Roman city of Solunto (Sicily, Italy). A selection of 16 well-contextualized samples was collected to represent different functions and building phases of this private house. The results show that a variety of locally available raw materials was used as aggregates and to produce binders. The diversity of raw materials' sources and production techniques identified in this study reveals the advanced technological knowledge of the builders of Solunto, indicating a complex relationship between the settlement's cityscape and its surrounding landscape.

KEYWORDS

building technology, Hellenistic–Roman period, mortars and plasters, petrography, raw materials, Solunto (Sicily), XRD, SEM-EDS

INTRODUCTION

Mortars and plasters are versatile materials whose study can yield important information regarding the use of raw materials and the development of building techniques in ancient times. Several studies have applied archaeometric approaches to characterize mortars and plasters, most notably lime-based ones, which were frequently used across various periods in world history (e.g., Lancaster, 2021; Maravelaki-Kalaitzaki et al., 2003; Schmölder-Veit et al., 2016). Most of these works focus on the mineralogical and chemical composition of mortars and plasters, as well as their mechanical properties (e.g., Genestar et al., 2006; Jackson et al., 2009) and were often tied to restoration projects (e.g.,

Funding information The authors acknowledge the Excellence Initiative (Eberhard Karls Universität Tübingen), Ministry for Science, Research, and Art of Baden-Württemberg, for their support during the preparation of this article.

This is an open access article under the terms of the Creative Commons Attribution License, which permits use, distribution and reproduction in any medium, provided the original work is properly cited.

© 2023 The Authors. *Archaeometry* published by John Wiley & Sons Ltd on behalf of University of Oxford.

14754754, 0, Downloaded from https://onlinelibrary.wiley.com/doi/10.1111/arcm.12853 by CNR GROUP 11 Istituto di Scienza dell', Wiley Online Library on [16/03/2023]. See the Terms and Conditions (https://onlinelibrary.wiley.com/terms-and-conditions) on Wiley Online Library for rules of use; OA articles are governed by the applicable Creative Commons License

Degryse et al., 2002; Faella et al., 2020). Other publications offer guidelines for their analysis (e.g., Artioli et al., 2019; Arizzi & Cultrone, 2021; Cantisani et al., 2022) or focus on raw material provenance and the technology of mortar production (e.g., Carò et al., 2008; Corti et al., 2016; De Luca et al., 2015; Pavía & Caro, 2008). Recent years have seen the emergence of mortar and plaster studies dealing with dating and related methodological issues (Daugbjerg et al., 2021; Dietzel & Boch, 2019; Schön et al., 2019; Toffolo, 2020). However, studies that interpret the results of scientific analysis on these materials within their environmental and archaeological context are still quite limited (e.g., Barone et al., 2004; Miriello et al., 2010; Montana et al., 2016, 2018, 2019; Schmölder-Veit et al., 2016; Schön et al., 2019). This study investigates human–environment interactions as well as building techniques through the analysis of the mortars and plasters from various building phases of the so-called *Ginnasio*, a luxurious private house, in the Hellenistic–Roman city of Solunto (fourth century BCE–third century CE). Due to their well-dated archaeological contexts and established building histories the city of Solunto as well as the *Ginnasio* present ideal conditions for an archaeometric study aimed at reconstructing past uses of the landscape. By applying a multipronged analytical approach combining thin-section petrography, X-ray micro- and powder diffraction as well as scanning electron microscopy (SEM), the results reconstruct mortar and plaster recipes used by the builders of this house and explore themes of technological transfer and innovation in one of the most important contexts for the study of urban development in the Hellenistic–Roman central Mediterranean.

Solunto and the so-called *Ginnasio*

The ancient city of Solunto (Figure 1a) was established by the Phoenicians in the area of Capo Solanto during the eighth century BCE (de Vincenzo, 2013; Wolf, 2003). Following the destruction of the city in the fourth century BCE, the settlement was rebuilt at another location, on Monte Catalfano. The foundation of this new settlement is dated *c*.307 BCE by Diodorus Siculus (Diod. 20.69.3–4), a chronology that is confirmed by the archaeological findings in the region (Wolf, 2003).

The *Ginnasio* is located at a crossroad, where the Via Cavallari crosses the main street Via dell'Agorà, which connects the entrance of the city and the *agora*. The *Casa con Atrium Tuscanicum* is located north of the *Ginnasio*. There may be another unexcavated house to the west. The house of interest, which was excavated *c*.1865, was erroneously identified as a gymnasium due to the discovery of an inscription of a gymnast on the street in front of the house (Portale, 2006; Sposito, 2014; Tusa, 1994; Wolf, 2003). It was later realized to be a private house (Wolf, 2003).

Due to the early date of the excavation, no stratigraphic data on the *Ginnasio* were published. Subsequently, only a few details, such as the wall painting (e.g., De Vos, 1975), were discussed. A systematic recording, however, did not take place for a long time. A first detailed architectural recording and reconstruction of the private house was carried out by Markus Wolf in 2003 (Wolf, 2003). He identified not only the functions of several rooms but also different building phases. These phases served as a guide for our sample selection. Even though the relative chronology is accepted, the date of origin for the house is still uncertain today. While Wolf, among others, assumes a first phase in the third century and a second phase in the second century BCE, others contend a first construction in the late second century BCE (e.g., Portale, 2006). In the meantime, the dating by Wolf of the third building phase in the late first century BCE is widely accepted (Wolf, 2003).

Geological background

The immediate surrounding of Solunto (Figure 2) is characterized by the lower Jurassic Fanusi Formation (Hettangium and Sinemurium) containing dolomitized breccias and dolorudites as well as doloarenites and dolosiltites of which comprise Monte Catalfano (Basilone, 2018). Part of these

14754754, 0, Downloaded from https://onlinelibrary.wiley.com/doi/10.1111/arcm.12853 by CNR GROUP 11 Istituto di Scienza dell', Wiley Online Library on [16/03/2023]. See the Terms and Conditions (https://onlinelibrary.wiley.com/terms-and-conditions) on Wiley Online Library for rules of use; OA articles are governed by the applicable Creative Commons License

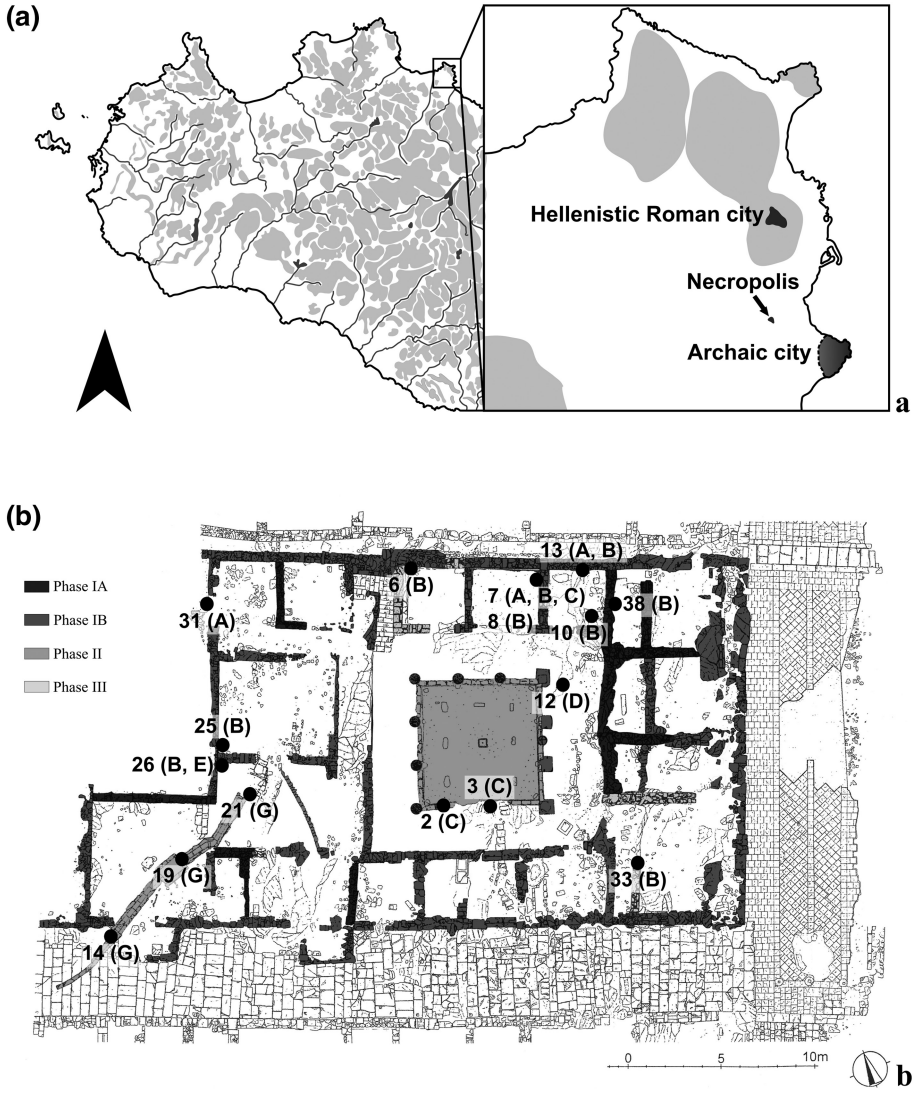

FIGURE 1 (a) Map of western Sicily (left) with a detail of the region around Solunto (right); and (b) plan of the phases of the *Ginnasio* with the indication of the sampling site and mortar/plaster types

formations is also the area between Monte Catalfano and Capo Zafferano, also called Cala dell'Osta, where calcite veins can be observed (Catalano et al., 2013). The wider area is also marked by the presence of Lower–Medium Pleistocene calcarenites intercalated with fossiliferous clays. These are part of the Marsala Synthem, which can be found along north-western Sicily. This formation is composed of whitish or yellowish calcarenites that are rich in mollusc fauna (gastropods and bivalves), but also corals alternate with carbonate marls and sandy marls with minor quantity of quartz and intercalations of thin pebbly conglomerates horizons. Furthermore, between Capo Zafferano and Capo Solanto, along the coastal area Upper Triassic cherty limestones of grey colour with radiolarites of the Scillato formation, can be found. Further in the inland pelites with manganesiferous nodules and silty clays, which are alternating with siltstone and fine-grained sandstone belonging to the Oligo-Miocene Numidian Flysch formation can be also observed. Finally other formations of Quaternary period rich in clays and sands are also marking the area around Monte Catalfano and the coastline (Catalano et al., 2013).

14754754, 0, Downloaded from https://onlinelibrary.wiley.com/doi/10.1111/arcm.12853 by CNR GROUP 11 Istituto di Scienza dell', Wiley Online Library on [16/03/2023]. See the Terms and Conditions (https://onlinelibrary.wiley.com/terms-and-conditions) on Wiley Online Library for rules of use; OA articles are governed by the applicable Creative Commons License

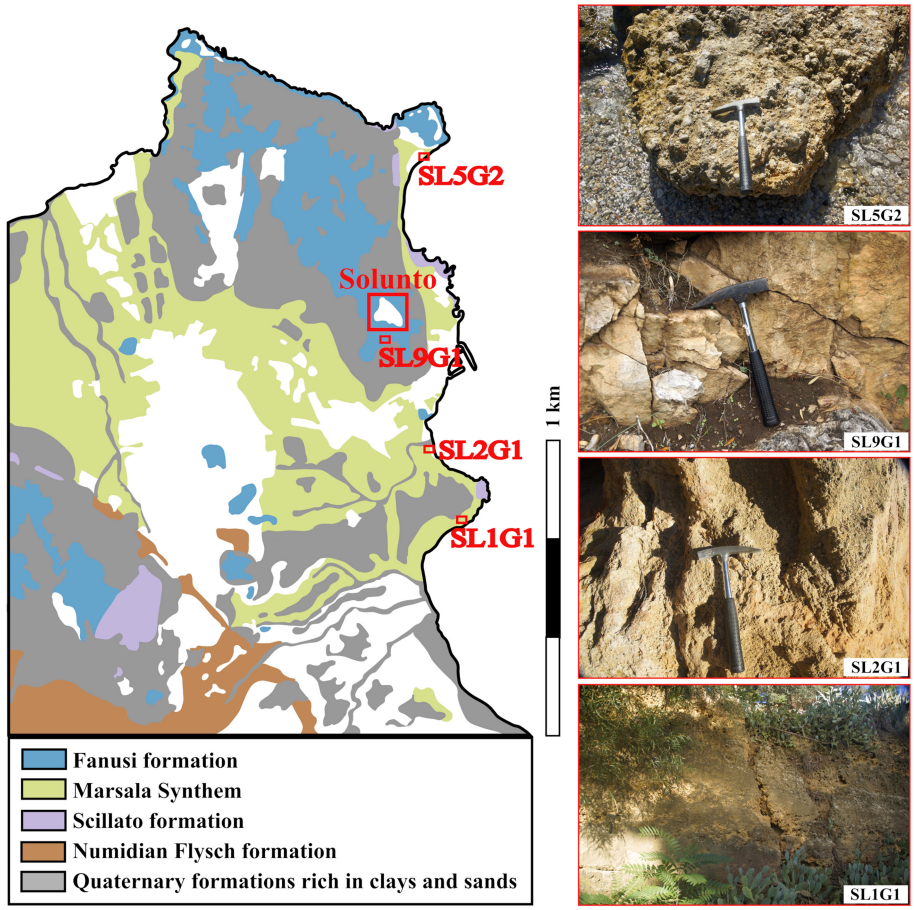

FIGURE 2 Simplified geological map (after Catalano et al., 2013) with the locations of the analysed outcrops of the Fanusi formation and Marsala Synthem. For the colour image, see wileyonlinelibrary.com

MATERIALS AND METHODS

A selection of mortar and plaster samples were collected in 2017 from three private houses of the Hellenistic–Roman city (Schön et al., 2019): the *Ginnasio*, the *Casa di Arpocrate* and the *Casa del Deposito a Volta* (Table 1; and additional supporting information S5). Sampling was carried out according to the building phases identified by Wolf (2003). The present study focuses on the *Ginnasio*, where 37 samples were selected to represent the first three building phases along with building materials of different functions—wall and floor plasters, and mortars such as pipe beddings. After a macroscopic evaluation, 16 (Figure 1b) partly multilayered specimens from the most secure contexts, in terms of relative chronology and function, were chosen to be further analysed using a multipronged approach. Although all samples were subject to thin-section petrography, a few representative samples were chosen for a more highly resolved mineralogical analysis via X-ray diffraction (XRD) as well as morphological and microstructural analysis using scanning electron microscope with energy dispersive spectroscopy (SEM-EDS).

In addition, four geological samples (three from the Marsala Synthem and one from the Fanusi Formation) were collected from the region of Solunto to characterize the raw materials that could be available for producing aggregates or binders. These geological samples were subject to petrographic analysis and X-ray powder diffraction (XRPD).

14754754, 0, Downloaded from https://onlinelibrary.wiley.com/doi/10.1111/arcm.12853 by CNR GROUP 11 Istituto di Scienza dell', Wiley Online Library on [16/03/2023]. See the Terms and Conditions (https://onlinelibrary.wiley.com/terms-and-conditions) on Wiley Online Library for rules of use; OA articles are governed by the applicable Creative Commons License

TABLE 1 Selected samples for archaeometric analysis.

Sample	Room	Architectural Element/ Function	Material	Sample Description	Type	Building phase (according Wolf 2003)	Petrography	μ-XRD²	XRPD	SEM
2	HG 4	Coating of the peristyle basin	Lime plaster	South side of the peristyle basin, inner site, western intercolumn	layer 1: C1	II	x	x		x
					layer 2: C2		x		x	x
					layer 2: inclusion: E		x	x		
3	HG 4	Coating of the peristyle basin	Lime plaster	South side of the peristyle basin, inner site, inner site, middle	C1	II	x		x	
6	HG 6	Coating of a wall	Lime plaster	North wall, western corner, lower section of the wall, 1st plaster (?)North wall, western corner, lower section of the wall, 1st plaster (?)	B1	IB	x		x	
7	HG 5	Coating of a wall	Lime plaster	Eastern wall, between northern corner and door closure, middle section, 2nd plasterEastern wall, between northern corner and door closure, middle section, 2nd plaster	layer 1: A2	III	x	x	x	
					layer 2: B4		x		x	x
					restauration: C2		x			
8	HG 5	Coating of a wall	Lime plaster	Eastern wall, between northern corner and door closure, middle section, 1st plasterEastern wall, between northern corner and door closure, middle section, 1st plaster	B1	IB	x	x	x	
10	HG 7	Floor	Lime plaster	South eastern corner, floor	layer 1: B3	I(?)	x		x	x
					layer 2: F		x	x	x	x
12	HG 4	Floor	Lime plaster	Eastern corridor of the peristyle, northern area, east side of the norther intercolumn, floor	D	III (?)	x	x	x	x
13	HG 7	Coating of a wall, wall mortar?	Lime plaster	Northern wall, lower section in the middle, 2nd plasterNorthern wall, lower section in the middle, 2nd plaster	layer 1: B4	III	x			
					layer 2: C2		x		x	

(Continues)

14754754, 0, Downloaded from https://onlinelibrary.wiley.com/doi/10.1111/arcm.12853 by CNR GROUP II Istituto di Scienza dell', Wiley Online Library on [16/03/2023]. See the Terms and Conditions (https://onlinelibrary.wiley.com/terms-and-conditions) on Wiley Online Library for rules of use; OA articles are governed by the applicable Creative Commons License

TABLE 1 (Continued)

Sample	Room	Architectural Element/ Function	Material	Sample Description	Type	Building phase (according Wolf 2003)	Petrography	μ-XRD²	XRPD	SEM
14	Next to OG 1	Bedding for a pipe	Lime mortar	Southern area in front of the room OG 1, on the street	G	II	x	x	x	
19	OG 1	Bedding for a pipe	Lime mortar	Northern side of the sedimentation basin	G	II	x		x	
21	OG 6	Wall for the pipe	Lime mortar	Northern end of the pipe, in front of the cistern	G	II	x		x	
25	OG 7	Coating of a wall	Lime plaster	South-western corner, lower section, 1st plaster	B1	IB	x		x	
26	OG 6	Coating of a wall	Lime plaster	North-western corner, lower section, 1st plaster	layer 1: B2	IB	x		x	
					layer 2: E		x			x
31	Next to OG 8	Floor	Lime plaster	Western area in front of the room OG 8, neighbour building, higher lever, 1st floor	A1	I	x		x	
33	LG 1	Coating of a wall	Lime plaster	Western wall, lower section in the middle	B6	III	x		x	x
38	LG 4	Wall mortar (?)	Lime mortar	Western wall, lower section in the middle	B5	III	x		x	

Room naming and building phases correspond to Wolf (2003).

14754754, 0, Downloaded from https://onlinelibrary.wiley.com/doi/10.1111/arcm.12853 by CNR GROUP II Istituto di Scienza dell', Wiley Online Library on [16/03/2023]. See the Terms and Conditions (https://onlinelibrary.wiley.com/terms-and-conditions) on Wiley Online Library for rules of use; OA articles are governed by the applicable Creative Commons License

Thin-section petrographic characterization

The 16 thin-sections were prepared and then analysed with a polarized light microscopy (PLM) using a Leica DM 2500P microscope at the Competence Center Archaeometry—Baden-Wuerttemberg (CCA-BW, University of Tübingen, Tübingen, Germany). This type of analysis allows for the characterization of primary components in mortars and plasters namely the aggregates and binders (Blaeuer & Kueng, 2007; Cantisani et al., 2022; Pavía & Caro, 2008; Pecchioni et al., 2020; Weber et al., 2009).

Observation of mortar and plaster thin sections reveals the composition of aggregates and therefore their likely provenance. In addition, the mean grain size, grain size distribution of aggregate, shape and the binder-to-aggregate ratio can give information about the processing (e.g., sieving and crushing) of raw materials as well as mortars and plasters preparation techniques (Pecchioni et al., 2020).

The study of binder in thin sections includes the characterization of the binder itself and of the lumps. The latter are described as whitish sometimes inconsistent grains (Bakolas et al., 1995; Bruni et al., 1997; Hughes et al., 2001). Their occurrence in lime-based mortars can be due to under- or over-burning of carbonate rocks during the firing process, lack of water during slaking and non-homogenous mixing of the binder materials with the aggregates (Cantisani et al., 2022; Leslie & Hughes, 2002). On the one hand, the observation of lumps related to under-burnt carbonate rocks in thin section identifies the type of carbonate rock burnt to prepare the lime. On the other hand, the observation of the binder itself provides information on its composition and texture (e.g., micritic, microsparitic) as well as structure (homogeneous, with lumps, in plagues), and the interaction with the aggregate. For example, the presence of reaction rims due to the addition of materials providing hydraulic characteristics such as pozzolana or ceramic (*cocciopesto*) (Arizzi & Cultrone, 2021).

X-ray diffraction (XRD)

To have a more detailed mineralogical characterization of particles that are not identifiable by the PLM, XRD was performed on a selection of uncovered thin sections and powdered materials. X-ray microdiffraction (μ-XRD^2) was performed on uncovered thin sections for a locally resolved analysis of the binder using a BRUKER D8 Discover X-ray microdiffractometer equipped with a Co-X-ray ($\lambda = 0.179$ nm) tube running at 30 kV/30 mA, a HOPG-primary monochromator, a 500 μm monocapillary optic with a 300 μm exit pinhole and a VÅNTEC-500 detector covering 40° in °2Theta and Chi at the CCA-BW in Tübingen, Germany. Typical measurement time for a diffractogram composed of two detector frames was 8 min. Samples were not rotated during measurement (Berthold et al., 2017; Schön et al., 2019). This technique allows highly resolved measurements focusing on small spot sizes below 1 mm^2, therefore making it possible to focus on precise points of the binder where aggregates from a macroscopic point of view are not visible. Nevertheless, in some cases it was impossible to analyse the pure binder as a high amount of fine-grained aggregates were presented within these samples.

Furthermore, X-ray powder diffraction (XRPD) was applied as a means of conducting a bulk analysis on a selection of representative samples and lumps present in the mortars and plasters. The latter were identified by using a stereomicroscope. However, for the samples of types E and F, it was impossible to separate lumps with the stereomicroscope. The analysis was run at the CNR Institute of Heritage Science (Florence Unit) using a X'Pert Pro PANalytical diffractometer equipped with an X'Celerator detector with a Cu X-ray tube ($\lambda = 0.154$ nm) and using a Ni-filtered Cu-Kα radiation source. The X-ray tube was operated at 40 kV and 30 mA. The diffraction patterns were collected from 3 to 70° 2θ with a step size of 0.02° and total time per pattern of 16 min 27 s. For phase identification of μ-XRD^2 and XRPD results the powder diffraction (PDF) database from the International Center for Diffraction Data (ICCD) was used.

14754754, 0, Downloaded from https://onlinelibrary.wiley.com/doi/10.1111/arcm.12853 by CNR GROUP 11 Istituto di Scienza dell', Wiley Online Library on [16/03/2023]. See the Terms and Conditions (https://onlinelibrary.wiley.com/terms-and-conditions) on Wiley Online Library for rules of use; OA articles are governed by the applicable Creative Commons License

Scanning electron microscopy with energy dispersive spectroscopy (SEM-EDS)

Microstructural and semi-quantitative chemical analyses of polished thin sections were obtained by means of a SEM-EDS (ZEISS EVO MA 15) with W filament equipped with analytical system in dispersion of energy EDS/SDD, Oxford Ultimax 40 (40 mm^2 with resolution 127 eV at 5.9 keV) with Aztec 5.0 SP1 software.

The measurements were performed on carbon-metallized thin sections of representative portions of the binder and lumps from each type, to study the microstructural characteristics of the selected samples and to identify the possible composition of the raw materials used to produce binders. Due to strong heterogeneity and porosity of the binder, for type A it was very difficult to identify pure areas of binder to analyse via SEM-EDS, which is why an investigation of this type was not possible. Both binders and lumps were analysed with the following operative conditions: an acceleration potential of 15 kV, 500 pA beam current, working distance comprised between 9.0 and 8.5 mm; 20 s live time as acquisition rate useful to archive at least 600.000 cts, on Co standard, process time four for point analyses; 500 µs pixel dwell time for maps acquisition with 1024 × 768 pixel resolution. EDS analyses were performed on several single spots of binders. The programme used for the microanalysis was an Aztec 5.0 SP1 software that employ the XPP matrix correction scheme developed by Pouchou and Pichoir (1991).

For all analysed types the hydraulicity index (HI) was calculated according to Boynton's formula $(SiO_2+Al_2O_3+Fe_2O_3)/(CaO+MgO)$ as ratio (Boynton 1980).

RESULTS

Archaeological materials

Petrographic observation

It was possible to identify seven petrographic types according to the textural and compositional features of the aggregates observed in the samples analysed. Some of these petrographic types can be subdivided into subtypes. These petrographic types are later referred to as mortar or plaster types. A summary of the results is provided in this section and for a detailed petrographic description, see the additional supporting information S1 and S2:

- *Shell-rich petrographic type A* (Figure 3a,b) is marked by abundant shells and can be divided in two subtypes. The first (Figure 3a; subtype A1) is characterized by the occurrence of coarse fossiliferous calcarenite fragments and shells, whereas the second (Figure 3b; subtype A2) contains a medium coarse quartz rich sand as well as shells. This type of material can be associated with wall plasters as well as floors and can be found in building phases 1 and 3.
- *Sand/gravel-rich petrographic type B* (Figure 3c) is the most common and it is marked by the addition of a sand/gravel, rich in quartz, chert and dolomite. This group is divisible into six subtypes based on variations in the coarseness, grain size distribution, shape, and sorting of the aggregates and the ratios of individual clasts relative to each other. Most of the samples of type B belong to wall plasters, only one of which comes from a floor plaster, and they can be found across the different building phases. More specifically, subtypes B1–B3 can be found in building phase 1, while B4–B6 can be related to building phase 3.
- *Ceramic-rich petrographic type C* (Figure 3d) is characterized by the presence of big angular crushed ceramic fragments and can be divided into two subtypes. Only coarse sherds can be detected in C1, whereas in C2 it is possible to observe both coarse and very fine ceramic fragments. These fragments of ceramics can be divided into two ceramic petrographic types. The first is dominated by quartz inclusions, while the second is marked by volcanic components (e.g.,

14754754, 0, Downloaded from https://onlinelibrary.wiley.com/doi/10.1111/arcm.12853 by CNR GROUP 11 Istituto di Scienza dell', Wiley Online Library on [16/03/2023]. See the Terms and Conditions (https://onlinelibrary.wiley.com/terms-and-conditions) on Wiley Online Library for rules of use; OA articles are governed by the applicable Creative Commons License

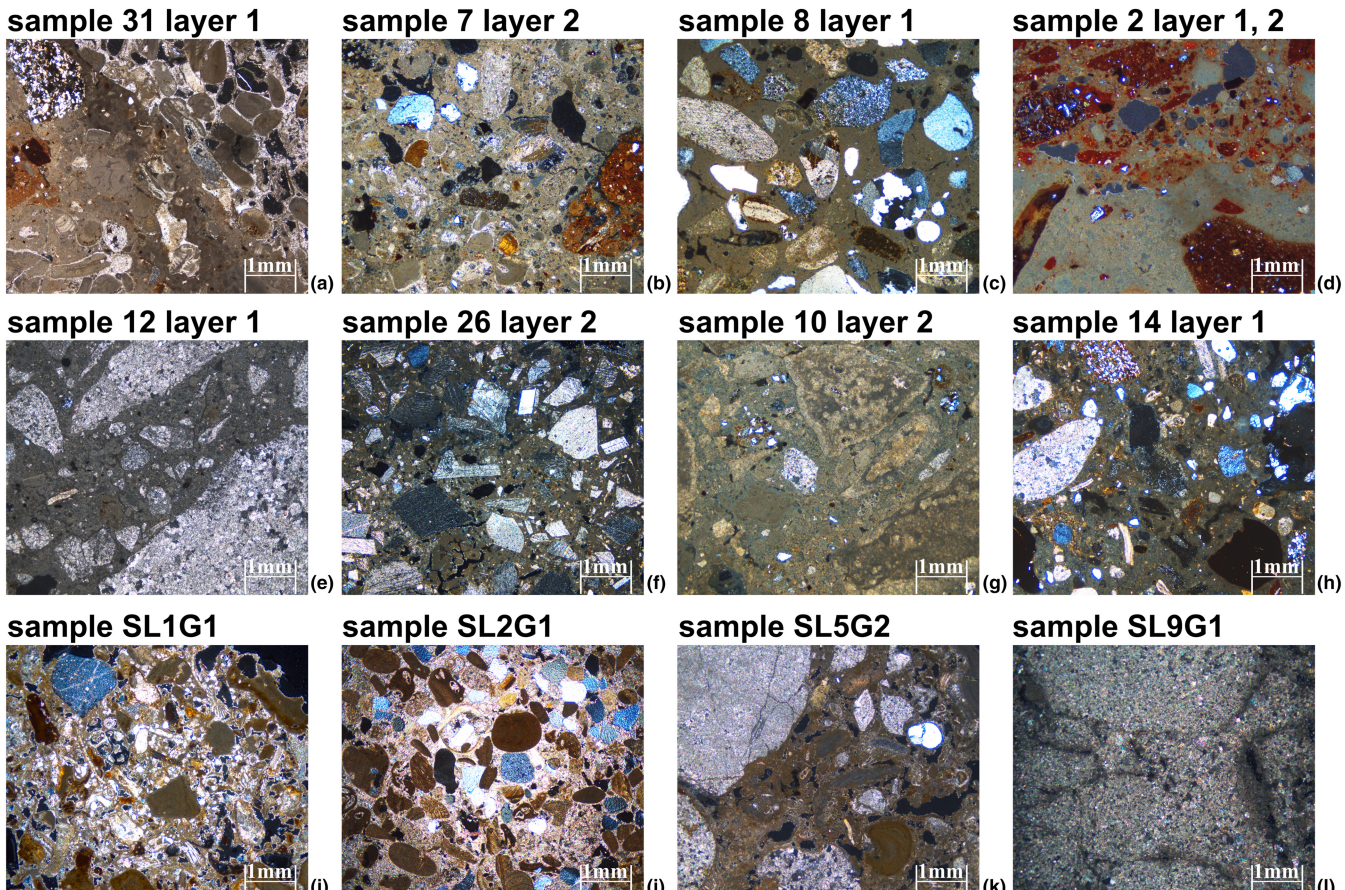

FIGURE 3 Thin-section micrographs of selected samples: (a) type A1; (b) type A2; (c) type B; (d) type C1 and C2; (e) type D; (f) type E); (g) type F; (h) type G; (i–k) Marsala Synthem (fossiliferous calcarenite); and (l) Fanusi formation (dolomite). Images taken under XP. For the colour image, see wileyonlinelibrary.com

14754754, 0, Downloaded from https://onlinelibrary.wiley.com/doi/10.1111/arcm.12853 by CNR GROUP II Istituto di Scienza dell', Wiley Online Library on [16/03/2023]. See the Terms and Conditions (https://onlinelibrary.wiley.com/terms-and-conditions) on Wiley Online Library for rules of use; OA articles are governed by the applicable Creative Commons License

fragments of basalts, pyroxenes and feldspars). Samples of type C are associated with different architectural elements: two of the samples belong to the peristyle basin, one is part of a wall mortar. Additionally, one of the specimens belongs to a restoration work; however, it is unclear whether this is ancient or modern. Only the samples of the peristyle basin can be related to building phase 2.

- *Dolomite-rich petrographic type D* (Figure 3e) is dominated by the presence of angular crushed dolomite fragments of different sizes. Only a small amount of other inclusion types can be observed. This single sample belonging to this petrographic type originates from a floor and cannot be associated with any specific building phase.
- *Calcite-rich petrographic type E* (Figure 3f) is marked by the addition of angular crushed calcite fragments to the binder. It can be found in two samples. One is a finishing layer of a plaster associated with building phase 1, the other is a recycled piece of mortar within another plaster type (type C) and must have been produced before that one.
- *Lump-rich petrographic type F* (Figure 3g) is only represented by one sample, and it is dominated by the presence of abundant lumps. Other inclusions such as quartz, dolomite and calcite can be observed as well, but less frequently. The sample is part of a finishing layer of a floor (see type D).
- *Heterogeneous sand rich petrographic type G* (Figure 3h) is marked by the addition of a polymictic poorly sorted sand/gravel. It is represented by three samples, which are all associated with a bedding for a water pipe and are belonging to building phase 2.

Results of XRD analysis

The μ-XRD[2] results (Figure 4a; and additional supporting information S3) show the presence of calcite in the binders of all samples. However, the analysis of the pure binder was often not possible as mentioned above; in addition, quartz was identified in types B, C and G. Aragonite was measured in types A and C, and dolomite in type D.

XRPD analysis carried out on the homogenized powders confirmed that calcite represents the main mineral phase in all mortar and plaster types (Figure 4b; and additional supporting information S3). This is in reference to both the binder and carbonate aggregates. Quartz was also detected in all samples, possibly related to the composition of aggregates. The presence of aragonite was also confirmed in types A and C, possibly stemming from the use of fossiliferous stone fragments (see below). In type C pyroxenes (augite), feldspars, hematite and micas were detected. These are most likely related to the ceramic fragments added to the binder. Finally, dolomite was detected, with a variable relative abundance, in almost all types.

The results of XRPD analyses performed on lumps Figure 4(c) and additional supporting information S3 show the presence of calcite and aragonite in types A and C. Dolomite and magnesite were detected in type D, while Mg compounds such as hydromagnesite and Mg hydroxides were found as abundant phases in lumps of type G.

Results of SEM-EDS analysis

SEM results complemented petrographic observations, showing the use of heterogeneous binders in each of the mortar and plaster samples studied. This is due to the presence of numerous lumps, connected to unmixed lime and under- as well as over-burnt rock fragments.

The EDS results show a variability in the weight percentage in all types (wt%; in the following all wt% are only given as numbers) of CaO, SiO_2, Al_2O_3 and MgO, probably due to the compositional heterogeneity of the rocks used to produce binders.

For type B, microchemical analyses of the binder in subtypes B3, B4 and B6 revealed a relatively high variability in the concentration of MgO (from 2.04 to 10.06), CaO (from 72.86 to 90.72), SiO_2 (from 2.25 to 8.54) and Al_2O_3 (from 1.07 to 1.63) (Table 2). In addition, the analysis of an under-burnt

14754754, 0, Downloaded from https://onlinelibrary.wiley.com/doi/10.1111/arcm.12853 by CNR GROUP 11 Istituto di Scienza dell', Wiley Online Library on [16/03/2023]. See the Terms and Conditions (https://onlinelibrary.wiley.com/terms-and-conditions) on Wiley Online Library for rules of use; OA articles are governed by the applicable Creative Commons License

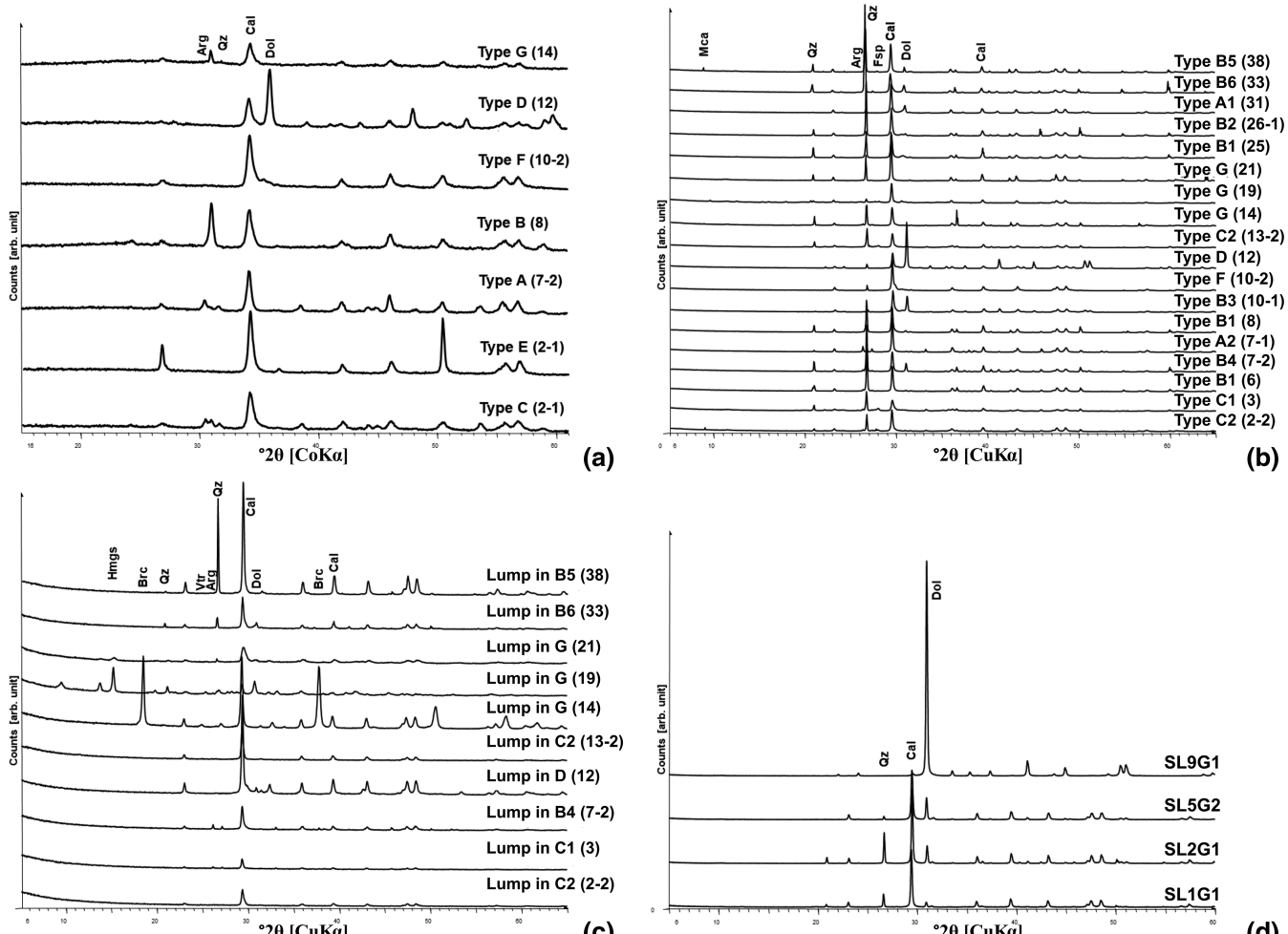

FIGURE 4 (a) μ-XRD[2] results of the binders; (b) XRPD results of the bulk analysis; (c) XRPD results of the lumps within the different mortar/plaster types; and (d) XRPD results of the geomaterials. Mineral abbreviations according to Whitney and Evans, 2010.

14754754, 0, Downloaded from https://onlinelibrary.wiley.com/doi/10.1111/arcm.12853 by CNR GROUP II Istituto di Scienza dell', Wiley Online Library on [16/03/2023]. See the Terms and Conditions (https://onlinelibrary.wiley.com/terms-and-conditions) on Wiley Online Library for rules of use; OA articles are governed by the applicable Creative Commons License

TABLE 2 Microchemical analysis results and hydraulic index (HI), bdl (below detection limit).

Type (sample)	*Spot*	*SiO_2*	*Al_2O_3*	*Fe_2O_3*	*MgO*	*CaO*	*Na_2O*	*K_2O*	*S_2O_3*	*Cl^-*	*Sum*	*HI*
B3 (10-1)	1	6.01	1.07	bdl	5.22	85.81	bdl	bdl	1.34	0.55	100	0.078
	2	6.94	1.34	bdl	10.06	81.65	bdl	bdl	bdl	bdl	100	0.090
	3	4.25	bdl	bdl	6.47	89.29	bdl	bdl	bdl	bdl	100	0.044
	4	8.37	1.29	bdl	9.99	80.36	bdl	bdl	bdl	bdl	100	0.107
B4 (7-2)	1	2.47	bdl	bdl	4.74	88.58	bdl	bdl	4.21	bdl	100	0.026
	2	3.36	bdl	bdl	2.93	90.72	bdl	bdl	2.43	0.56	100	0.036
	3	7.19	bdl	bdl	2.04	79.46	1.40	bdl	7.37	2.54	100	0.088
	4	2.25	bdl	bdl	2.40	92.68	bdl	bdl	2.67	bdl	100	0.024
B6 (33)	1	4.03	bdl	bdl	5.27	84.93	bdl	bdl	5.03	0.74	100	0.045
	2	8.71	bdl	bdl	8.79	72.86	bdl	bdl	8.40	0.41	100	0.107
	3	4.22	bdl	bdl	4.29	85.68	bdl	bdl	4.98	0.83	100	0.047
	4	8.54	1.63	bdl	4.74	76.58	1.18	bdl	6.55	0.78	100	0.125
C1 (2-1)	1	21.34	3.77	bdl	16.22	54.97	bdl	0.80	2.19	0.71	100	0.353
	2	21.75	3.35	bdl	20.62	47.02	1.24	1.33	3.75	0.94	100	0.371
	3	12.07	2.62	bdl	10.65	69.82	1.22	bdl	3.62	bdl	100	0.183
	4	10.43	1.74	bdl	12.13	74.55	bdl	0.62	bdl	0.53	100	0.140
	5	18.42	3.00	bdl	16.28	58.12	bdl	0.75	2.79	0.64	100	0.288
C2 (2-2)	1	7.21	1.83	bdl	6.62	82.99	bdl	bdl	1.36	bdl	100	0.101
	2	20.06	4.72	bdl	11.71	61.68	bdl	bdl	1.83	bdl	100	0.338
	3	9.88	2.08	bdl	4.04	81.39	bdl	bdl	2.59	bdl	100	0.140
	4	17.63	5.36	1.78	12.41	61.23	bdl	bdl	1.59	bdl	100	0.336
	5	11.96	3.66	bdl	9.24	73.17	bdl	bdl	1.97	bdl	100	0.190
D (12)	1	2.80	bdl	bdl	9.23	73.30	bdl	bdl	8.30	6.37	100	0.034
	2	3.12	1.47	bdl	10.74	76.90	bdl	bdl	6.95	0.82	100	0.052
	3	3.91	bdl	bdl	4.66	82.92	bdl	bdl	7.79	0.72	100	0.045
	4	2.69	1.35	bdl	2.45	93.51	bdl	bdl	bdl	bdl	100	0.042
E (26-2)	1	bdl	bdl	bdl	bdl	100.00	bdl	bdl	bdl	bdl	100	0.000
	2	bdl	bdl	bdl	4.41	93.03	bdl	2.55	bdl	bdl	100	0.000
	3	bdl	bdl	bdl	17.91	80.94	bdl	1.15	bdl	bdl	100	0.000
	4	bdl	bdl	bdl	28.09	71.91	bdl	bdl	bdl	bdl	100	0.000
F (10-2)	1	6.01	1.07	bdl	5.22	85.81	bdl	bdl	1.33	0.55	100	0.078
	2	6.94	1.34	bdl	10.06	81.65	bdl	bdl	bdl	bdl	100	0.090
	3	4.25	bdl	bdl	6.47	89.29	bdl	bdl	bdl	bdl	100	0.044

fragment of rock in sample 33 (and see additional supporting information S4, g–i) revealed a mean concentration of 85.23 of CaO, 3.28 of SiO_2 and 7.83 of MgO. This implies the use of a carbonate rock, containing Ca and Mg phases, to produce this binder. Conversely, high variability in the concentrations of major elements was recorded in samples belonging to type C (Table 2). It is remarkable that higher concentrations are detectable for SiO_2 (for C1: from 10.43 to 21.75; for C2: from 7.21 to 20.06) and Al_2O_3 (for C1: from 1.74 to 3.77; for C2: from 1.83 to 5.36).

In contrast, a low concentration of SiO_2 and Al_2O_3 were detected in the binder of representative samples of types D and F, with a variable concentration of MgO, ranging from 2.45 to 10.74 for type D and from 5.22 to 10.06 for type F. For sample 10-2 (type F) the SEM-EDS map of the distribution of Ca and Mg in an area of 3 × 2 mm is shown (and see additional supporting information S4, a–c).

14754754, 0, Downloaded from https://onlinelibrary.wiley.com/doi/10.1111/arcm.12853 by CNR GROUP 11 Istituto di Scienza dell', Wiley Online Library on [16/03/2023]. See the Terms and Conditions (https://onlinelibrary.wiley.com/terms-and-conditions) on Wiley Online Library for rules of use; OA articles are governed by the applicable Creative Commons License

A higher amount of CaO and a smaller amount of MgO can be observed, which can be related to the usage of a carbonate rock for binder production.

For type E in layer 2 in sample 26 (Table 2), only CaO and MgO and small amount of K_2O were detected in the analysed spots of the binder. The MgO amount ranges from 4.41 to 28.09, indicating once again the use of a carbonate rock containing Ca and Mg phases to produce the binder.

A somewhat different picture can be drawn for type G, where a microstructural and compositional heterogeneity can be observed. The mapping of an area within sample 14 (and see additional supporting information S4, d–f) shows a relatively higher concentration of Mg in the most porous areas of the binder and in the lumps. These observations are consistent with our XRPD analyses that showed an abundance of Mg compounds.

The calculation of HI shows that only in the samples of type C, characterized by the addition of ceramic, is this value, ranging from 0.10 to 0.35, compatible to mortars with low/medium hydraulicity (Table 2).

Geological materials

Petrographic observations and XRPD results

Three samples of the Marsala Synthem and one of the Fanusi Formation were analysed to determine the raw materials used for the binder as well as aggregates production of the mortars and plaster. Although the first three samples belong to the same formation (Marsala Synthem), they differ in their petrographic and mineralogical compositions.

- *SL1G1* (Figure 3i) is dominated by partly well-preserved shells and corals within a calcitic matrix. Quartz and smaller amounts of subrounded chert and dolomite fragments are also present. These observations were complemented by XRPD analysis that showed the presence of calcite, quartz and dolomite (Figure 4d; and additional supporting information S3).
- *SL2G1* (Figure 3j) is marked by rounded clasts of quartz, shells and coral as well as dolomite within a calcitic matrix. As in the previous sample, XRPD (Figure 4d; and additional supporting information S3) analysis showed the presence of calcite, quartz and dolomite.
- *SL5G2* (Figure 3k) is characterized by the presence of dolomite fragments with different sizes within a calcitic matrix. Additionally, shells and corals can be observed. Here, the XRPD analyses (Figure 4d; and additional supporting information S3) yielded not only calcite but also quartz and dolomite.
- In *SL9G1* (Figure 3l) dolomite could be detected via petrographic observation and XRPD (Figure 4d; and additional supporting information S3).

DISCUSSION

Aggregates: Source of raw materials

The petrography and mineralogy of both archaeological and geological samples in this study indicates that most of the raw materials for aggregates can be found in the immediate surrounding of Solunto. The ancient city is built on top of the Fanusi Formation, which is presumably the origin of the dolomite used in type D. While the city structures are partly cut into this bedrock, the dolomite debris deriving from building activities was likely an abundant raw material that became incorporated into mortar and plaster production. The angularity of dolomite grains in thin section implies that it was crushed during the production process. Calcite fragments in type E may also originate from the Faunsi formation (see above).

Aggregates used for types A2, B and G may originate from sands and gravels that are especially abundant in the quaternary formations present around Monte Catalfano and in the coastline. Differ-

14754754, 0, Downloaded from https://onlinelibrary.wiley.com/doi/10.1111/arcm.12853 by CNR GROUP 11 Istituto di Scienza dell', Wiley Online Library on [16/03/2023]. See the Terms and Conditions (https://onlinelibrary.wiley.com/terms-and-conditions) on Wiley Online Library for rules of use; OA articles are governed by the applicable Creative Commons License

ences in the roundness, grain-size distribution, sorting and composition of these sediments could suggest varied sources and processing techniques (e.g., sieving).

Type A2 shows evidence for the use of fossiliferous calcarenite as an aggregate which is a typical rock of the Marsala Synthem, as also our analysis showed (see above). The latter outcrops in the area surrounding Monte Catalfano but is not directly available on the site. It has been already noted (De Vos, 1975; Wolf, 2003) that this type of rock was used as building material in several structures of Solunto including the *Ginnasio*. Calcarenite is advantageous to use as it is a more easily workable material in comparison to the local dolomite. In this case, calcarenite was likely available in the city of Solunto as debris from other building activities, or as a material that was intentionally brought to the city to produce mortars and plasters. It is also possible that the lime production occurred close to the sources of calcarenite, and that the building materials were transported to the city, as will be discussed below.

Moving to type C, which is marked by the occurrence of ceramic fragments, and representing mortar and plaster known as *cocciopesto*. The sherds used as aggregates show different petrographic characteristics that point to various origins. One ceramic petrographic type is rich in quartz and marked by the presence of thermally altered microfossils and may therefore be of local or 'intra-island' origin (Montana et al., 2009). The second type, with volcanic inclusions, could be associated with imports, potentially the Campana A, as it was already suggested in the study of a similar type of mortar from the *Casa di Arpocrate* (Schön et al., 2019), based on the ceramic studies carried out by Montana et al. (2009). It is therefore possible that broken sherds of pottery used in Solunto were recycled to produce a reddish coloured and/or slightly hydraulic mortar. This is indicated by the calculated hydraulic index which shows an increased Si/Al/Fe-content relative to the other binders.

Finally, type F deserves a separate discussion. Here it is not clear if rare inclusions, such as quartz, dolomite and arenite, were intentionally added or if they derived from the binder production process. It is possible that a doloarenite or dolosiltite, which are also of local origin, were used to produce a binder of this plaster type and that the inclusions are remnants from the binder production process.

Binder: Source of raw materials

The results suggest that various types of raw materials were used to produce binders. Those in types B and C may have been produced by using calcarenite. This is indicated by the detection of calcite in the lumps of samples 2 (type C1), 33 (type B6) and 38 (type B5). This mineral is also the main component of the locally available calcarenite.

These types, as well as type A, featured a weak peak of aragonite along with calcite, for example, in samples 7 (types A2 and B4) and 3 (type C1). Since aragonite was not detected in the XRPD analysis of neither geological samples nor the fossilized shells of calcarenite, its presence in the binders requires an alternative explanation. Our results showed that three samples of calcarenite analysed contain a variable amount of dolomite. The presence of Mg ions such as in dolomite can lead to the formation of aragonite alongside calcite during the mortar and plaster hardening process (Lippmann, 1973; for the detection of aragonite and calcite in dolomitic mortars, see Diekamp et al., 2008, 2009). It is also possible that crushed shells from the coastline were used to produce these types of binders in addition to the use of fossiliferous calcarenite. The former are normally composed of aragonite, and they were surely abundant in a city placed near the sea. When used as raw material for binders, it is possible that they are not completely transformed to quick lime during the burning process, which means aragonite is still detectable. The use of shells to produce lime is also a well-known practice in ancient times (Artioli et al., 2019).

The binder in type D could have been produced from a fossiliferous calcarenite as well. The presence of dolomite and magnesite, in addition to calcite, may also be related to the use of sources containing Mg-rich rocks, which is supported by our observations of geological samples (see above). Similar observations have been made in binders of types E and F where MgO has been detected in addition to a high concentration of CaO (Table 2).

14754754, 0, Downloaded from https://onlinelibrary.wiley.com/doi/10.1111/arcm.12853 by CNR GROUP 11 Istituto di Scienza dell', Wiley Online Library on [16/03/2023]. See the Terms and Conditions (https://onlinelibrary.wiley.com/terms-and-conditions) on Wiley Online Library for rules of use; OA articles are governed by the applicable Creative Commons License

Finally, type G may have been produced by firing a Mg-rich rock, such as dolomite (Diekamp et al., 2008; Kitamura, 2001), or a fossiliferous calcarenite with a much higher amount of Mg-rich rocks. This is suggested by the detection of mineral phases such as brucite within sample 14 (type G), and hydromagnesite in samples 19 and 21 (type G). Generally, well-preserved Mg lime binders can be observed in several ancient buildings in terrestrial and marine conditions (Cantisani et al., 2021; Diekamp et al., 2009; Mannoni et al., 2006; Moropoulou et al., 1993; Pavía et al., 2005; Schork, 2012).

The firing of a Mg-rich rock in lime production often yields both CaO and MgO. During the slaking process through the addition of water, portlandite and brucite form from highly reactive CaO and the less soluble MgO, respectively. While portlandite converts back to $CaCO_3$ during the hardening process, brucite is poorly soluble. This leads to a delayed formation of hydrocarbonates such as hydromagnesite, nesoqueonite and artinite. These hydro phases can also hinder the formation of magnesite (Atzeni et al., 1996; Beruto et al., 1998; Chever et al., 2010; Diekamp et al., 2009; Pecchioni et al., 2020).

The lumps of type G show a clear segregation of Mg phases, such as hydromagnesite and Mg oxides, which can be explained by the formation of Ca carbonate and Mg carbonate crystals (Cantisani et al., 2022; Diekamp et al., 2009). The poorly soluble brucite in sample 14 may be the result of exposure under water or high humidity (Cantisani et al., 2022). This sample was part of a bedding for a water channel, where during heavy rainfall the water is still nowadays stored and transported.

The use of calcarenite and dolomite in binder production is consistent with our observations in the study of aggregates at Solunto. Both types of rocks have different advantages in their material properties and availability. As mentioned above, dolomite is immediately available in Solunto and, in addition, it is a relatively hard material, which, according to Vitruvius, is an ideal feature for making mortars (Vitr., *De arch*. 2.5.1). Interestingly, in Solunto dolomitic binders seem to be associated with mortars rather than plasters. The latter seem to be made generally from calcarenite, that has the advantage of being a much softer and porous material that is, according to Vitruvius, more suitable for plaster production (Vitr., *De arch*. 2.5.1).

Even if calcarenite was not directly available in the city, the advantages that this material offers could be the reason that it was brought to Solunto. On the other hand, it is not possible to rule out that the actual calcarenite-based lime was brought to the city with amphorae from production areas located in the hinterland of Solunto (De Luca et al., 2015; Schön, 2015). Unfortunately, in absence of identified production installations, both in Solunto and the countryside, it is not possible to confirm this hypothesis and both scenarios should be considered.

Binders made from calcarenite can also be observed in Palermo, a city that was also founded by the Phoenicians. However, this nearby city is built over the Marsala Synthem and therefore it is not surprising that the directly available rock was also used here to produce mortars and plasters (Montana et al., 2016). Nevertheless, it is not possible to exclude that the use of calcarenite as an ideal source for buildings materials was a well-known practice in the wider area of its occurrence.

Mortar and plaster recipe development

Changes in recipe, pointing to technological advances and a continuous development, become particularly visible through the combination of the petrographic results and the relative chronology of the archaeological context.

Type B, which was applied in various building phases as a wall plaster, is particularly interesting in terms of recipe development. Samples generally show a decrease in the size of inclusions and an increase in the abundance of inclusions over time. Where earlier phases are marked by medium- to large-sized inclusions and later phases show a decrease in the size of individual grains, but an increase in their frequency. This leads to a shift in the binder-to-aggregate ratio. Diachronic changes are particularly noticeable in room HG5. Here, sample 8 was used to investigate the first wall painting phase and sample 7 to investigate the second phase. While sample 8 shows medium-sized aggregates,

14754754, 0, Downloaded from https://onlinelibrary.wiley.com/doi/10.1111/arcm.12853 by CNR GROUP 11 Istituto di Scienza dell', Wiley Online Library on [16/03/2023]. See the Terms and Conditions (https://onlinelibrary.wiley.com/terms-and-conditions) on Wiley Online Library for rules of use; OA articles are governed by the applicable Creative Commons License

only smaller ones can be found in sample 7. The systems for applying these mortars and plasters also differ. The first phase shows the use of a single-layer system, whereas the second phase a multilayer system. A single-layer systems consists of one type of mortar and plaster that is applied in one or several layers. A multilayer system uses at least two different types of mortars and plasters in one building phase. These layers can be associated with each other via inclusions or by a diffuse contact zone (Schön, 2015). Since the latter method can achieve the same layer thickness as the single-layer system, it is not surprising that smaller aggregates were used here. However, in other samples that can be assigned to a later phase (e.g., samples 33, 38) and do not show a multilayer system, the maximum grain size is significantly smaller, and the proportion of aggregates is increased compared to the samples of the earlier phase. In conclusion, it seems that the grain sizes within plasters decreases, while the number of aggregates increase, which results in a lower proportion of binder. Consequently, these results show a change in the recipe over a longer period. This has not yet been demonstrated to occur in other locations (Genestar et al., 2006; Ricca et al., 2019; Schmölder-Veit et al., 2016). It is possible that the reduction of the amount of binder also served to lower the manufacturing costs. As the production of the lime needs a lot of resources (time, wood, manpower), it will also have accounted to the largest proportion of the costs (Gotti et al., 2008; Lancaster, 2021).

CONCLUSIONS

The results of this combined study on the mortar and plaster samples of the *Ginnasio* in Solunto shed new light on the building technology of this city. Based on the aggregates it could be shown that seven different types of mortars and plasters were used in this private house. In addition, our results suggest that a variety of raw materials were used to produce the binders too. Nevertheless, all necessary raw materials for the mortars and plasters have their origin in the area around Solunto. Only some pottery fragments do not have a local origin, but they were most certainly recycled within the mortars and plasters and were not imported to be used as aggregates. The use of raw materials marked by different properties demonstrates a good knowledge of local sources by the ancient builders of Solunto and highlights a variety of technological choices whose meaning should be explored in a more extensive study. It is interesting to note that, apart from type G, which was used exclusively as embedding material for a water pipe, there no strict correlation between these mortar and plaster types to their function. However, there seems to be a tendency for type B (sand/gravel-rich petrographic type) to be associated with plasters. This means that at this stage we cannot produce a functional explanation for the variability in natural resources and technology. Due to our sampling being conducted in accordance with the well-documented building phases, it was also possible to identify recipe changes within plaster type B. The change can may be related to a reduction in production costs, as discussed above.

The microchemical, mineralogical and petrographic analyses of well contextualized mortars and plasters are useful tools for understanding the choice and evolution of strategies of raw materials procurement, technologies used for the preparation of building materials as well as their application. Ultimately this helps us to evaluate the knowledge and use of the resources in the surrounding landscape, and to trace different forms of cultural expression of ancient civilisations.

AUTHOR CONTRIBUTIONS

B.B.: conceptualization, methodology, formal analysis (μ-XRD^2, XRPD, petrography), investigation, writing original draft, review and editing the final draft, visualization. S.A.: conceptualization, methodology, supervision of the project and formal analysis (petrography and XRD), writing, review, and editing original and final draft. F.S.: conceptualization, supervision and administration of the project, review of the original and final draft, visualization, funding acquisition. E.C.: methodology, formal analysis (XRPD and SEM-EDS analyses), writing original draft, review and editing final draft, visualization. C.B.: methodology, supervision of formal analysis (μ-XRD^2, XRPD), review and editing of the final draft, resources.

14754754, 0, Downloaded from https://onlinelibrary.wiley.com/doi/10.1111/arcm.12853 by CNR GROUP 11 Istituto di Scienza dell', Wiley Online Library on [16/03/2023]. See the Terms and Conditions (https://onlinelibrary.wiley.com/terms-and-conditions) on Wiley Online Library for rules of use; OA articles are governed by the applicable Creative Commons License

ACKNOWLEDGEMENTS

This article is based on an MA thesis in Classical Archaeology (Eberhard Karls Universität Tübingen) by Beatrice Boese, supervised by Silvia Amicone, Christoph Berthold, Thomas Schäfer and Frerich Schön. This work was carried out in the framework of an interdisciplinary collaboration between the Institute of Classical Archaeology, the SFB 1070 ResourceCultures and the Competence Center Archaeometry—Baden-Wuerttemberg (CCA-BW). The authors thank the Polo Regionale di Palermo per i Parchi e I Musei Archeologici, the Museo Antonio Salinas in Palermo, the Parco Archeologico di Solunto and the Centro di Servizi di Microscopia Elettronica e Microanalisi (MEMA), University of Florence. In addition, for their help and feedback, the authors thank Stefano Cespa, Ada Dinckal, Leonhard Geißler, Lars Heinze, Arvin Raj Mathur, Giuseppe Montana, Lauren Osthof, Kai Riehle, Hanni Schön, Johannes Seidler and Linda Stoeßel. Finally, the authors would also like to acknowledge the Excellence Initiative (Eberhard Karls Universität Tübingen), the Ministry for Science, Research, and Art of Baden-Württemberg, for their support during the preparation of this article. Constructive comments by anonymous reviewers and the editor helped us strengthen the paper and are much appreciated.

Open Access funding enabled and organized by Projekt DEAL.

DATA AVAILABILITY STATEMENT

The additional data that support the findings of the study are openly available at https://doi.org/10.7910/DVN/KTDGD9.

ORCID

Silvia Amicone https://orcid.org/0000-0001-8237-7044
Emma Cantisani https://orcid.org/0000-0002-4909-5624

REFERENCES

Arizzi, A., & Cultrone, G. (2021). Mortars and plaster—How to characterise hydraulic mortars. *Archaeological and Anthropological Sciences*, *13*, 144. https://doi.org/10.1007/s12520-021-01404-2

Artioli, G., Secco, M., & Addis, A. (2019). The Vitruvian legacy: Mortars and binders before and after the Roman world. *EMU Notes in Mineralogy*, *20*, 151–202. https://doi.org/10.1180/EMU-notes.20.4

Atzeni, C., Massidda, L., & Sanna, U. (1996). Magnesian limes. Experimental contribution to interpreting historical data. *Science and Technology for Cultural Heritage*, *5*(2), 29–36.

Bakolas, A., Biscontin, G., Moropoulou, A., & Zendri, E. (1995). Characterization of the lumps in the mortars of historic masonry. *Thermochimica Acta*, *269*(270), 809–816. https://doi.org/10.1016/0040-6031(95)02573-1

Barone, G., Branca, C., Gresta, S., Imposa, S., Leone, A., & Majolino, D. (2004). Geoarcheometric and geophysical methodologies applied to the study of cultural heritage: '*St. Agata la Vetere*' in Catania (Sicily, Italy). *Journal of Cultural Heritage*, *5*(1), 263–271.

Basilone, L. (2018). *Lithostratigraphy of Sicily*. Springer.

Berthold, C., Zimmer, K. B., Scharf, O., Koch-Bringmann, U., & Bente, K. (2017). Nondestructive, optical and X-ray analytics with high local resolution on ATTIC white-ground lekythoi. *Journal of Archaeological Science: Reports*, *16*, 513–520. https://doi.org/10.1016/j.jasrep.2016.02.008

Beruto, D., Botter, R., Casarino, A., Fieni, L., Giordani, M., La Rosa, C., Mannoni, T., & Vecchiattini, R. (1998). New laboratory researches to produce lime putty with controlled microstructure. *Compatible Materials for Protection. P.a.C.T*, *56*(2), 131–140.

Blaeuer, C., & Kueng, A. (2007). Examples of microscopic analysis of historic mortars by means of polarising light microscopy of dispersions and thin sections. *Materials Characterization*, *58*, 1199–1207. https://doi.org/10.1016/j.matchar.2007.04.023

Boynton, R. S. (1980). *Chemistry and Technology of Lime and Limestone*. John Wiley & Sons, New York.

Bruni, S., Cariati, F., Fermo, P., Cairati, P., Alessandrini, G., & Toniolo, L. (1997). White lumps in fifth- to seventeenth-century AD mortars from northern Italy. *Archaeometry*, *39*(1), 1–7. https://doi.org/10.1111/j.1475-4754.1997.tb00786.x

Cantisani, E., Fratini, F., & Pecchioni, E. (2022). Optical and electronic microscope for Minero-petrographic and microchemical studies of lime binders of ancient mortars. *Minerals*, *12*(1), 41. https://doi.org/10.3390/min12010041

Cantisani, E., Fratini, F., Vettori, S., Pecchioni, E., Chelazzi, L., & Arrighetti, A. (2021). Mineralogical and petrographic study of building materials from the Argentario coastal towers (Tuscany, Italy): Anthropic evidence of the ancient landscape. *Italian Journal of Geosciences*, *140*(1), 155–166. https://doi.org/10.3301/IJG.2020.27

Carò, F., Riccardi, M. P., & Mazzilli Savini, M. T. (2008). Characterization of plasters and mortars as a tool in archaeological studies: The case of Lardirago Castle in Pavia, northern Italy. *Archaeometry*, *50*(1), 85–100.

14754754, 0, Downloaded from https://onlinelibrary.wiley.com/doi/10.1111/arcm.12853 by CNR GROUP 11 Istituto di Scienza dell', Wiley Online Library on [16/03/2023]. See the Terms and Conditions (https://onlinelibrary.wiley.com/terms-and-conditions) on Wiley Online Library for rules of use; OA articles are governed by the applicable Creative Commons License

Catalano, R., Avellone, G., Basilone, L., Contino, A., & Agate, M. (2013). Note illustrative della Carta geologica d'Italia alla scala 1:50.00 e note illustrative del Foglio 595—Palermo. In Servizio Geologico d'Italia ISPRA (Ed.). Rome.

Chever, L., Pavía, S., & Howard, R. (2010). Physical properties of magnesian lime mortars. *Materials and Structures*, *43*, 283–296. https://doi.org/10.1617/s11527-009-9488-9

Corti, C., Rampazzi, L., & Visonà, P. (2016). Hellenistic mortar and plaster from Contrada Mella near Oppido Mamertina (Calabria. Italy). *International Journal of Conservation Science*, *7*(1), 57–70.

Daugbjerg, T. S., Lindroos, A., Heinemeier, J., Ringbom, Å., Barrett, G., Michalska, D., Hajdas, I., Raja, R., & Olsen, J. (2021). A field guide to mortar sampling for radiocarbon dating. *Archaeometry*, *63*(5), 1121–1140. https://doi.org/10.1111/arcm.12648

De Luca, R., Miriello, D., Pecci, A., Domínguez-Bella, S., Bernal-Casasola, D., Cottica, D., Bloise, A., & Crisci, G. M. (2015). Archaeometric study of mortars from the Garum shop at Pompeii, Campania, Italy. *Geoarchaeology: An International Journal*, *30*, 330–351. https://doi.org/10.1002/gea.21515

de Vincenzo, S. (2013). Bemerkungen zur Urbanistik und Kultaspekten der Stadt Solunt in punischer und römischer Zeit. *Mediterraneo Antico*, *16*(2), 767–794.

De Vos, M. (1975). Pitture e mosaico a Solunto. *Bulletin. Antieke Beschaving*, *50*, 195–224.

Degryse, P., Elsen, J., & Waelkens, M. (2002). Study of ancient mortars from Sagalassos (Turkey) in view of their conservation. *Cement and Concrete Research*, *32*, 1457–1463. https://doi.org/10.1016/S0008-8846(02)00807-4

Diekamp, A., Konzett, J., & Mirwald, P. W. (2009). Magnesian lime mortars—Identification of magnesium-phases in medieval mortars and plasters with imagine techniques. In B. Middendorf, A. Just, D. Klein, A. Glaubitt, & J. Simon (Eds.), *12th Euroseminar on microscopy applied to building materials* (pp. 309–317). Technische Universität Dortmund.

Diekamp, A., Konzett, J., Wertl, W., Tessadri, R., & Mirwald, P. W. (2008). Dolomitic lime mortar—A commonly used building material for medieval buildings in western Austria and northern Italy. In J. W. Lukaszewicz, P. Niemcewicz (Eds.): Proceedings of the 11th International Congress on Deterioration and Conservation of Stone. Torun, Poland, 15–20 September 2008 (I), pp. 579–604.

Dietzel, M. & Boch, R. (2019). Radiometrische Altersdatierung von Historischem Kalkmörtel. In B. Hebert (Ed.): St. Johann im Mauerthale und Ybbs an der Donau. Zwei neu entdeckte römische Militäranlagen am norischen Limes und ihre Nachfolgebauten. Horn-Wien (Fokus Denkmal, 11), pp. 229–233.

Faella, G., Aurilio, M., Tafuro, A., & Frunzio, G. (2020). Natural Pozzolanic mortars for cultural heritage. *International Journal of Advanced Research in Engineering and Technology (IJARET)*, *11*(10), 282–296.

Genestar, C., Pons, C., & Más, A. (2006). Analytical characterisation of ancient mortars from the archaeological Roman city of Pollentia (Balearic Island, Spain). *Analytica Chimica Acta*, *557*, 373–379. https://doi.org/10.1016/j.aca.2005.10.058

Gotti, E., Oleson, J. P., Bottalico, L., Brandon, C., Cucitore, R., & Hohlfelder, R. L. (2008). A comparison of the chemical and enineering characteristics of ancient roman hydraulic concrete with a modern reproduction of vitruvian hydraulic concrete. *Archaeometry*, *50*(4), 576–590. https://doi.org/10.1111/j.1475-4754.2007.00371.x

Hughes, J., Leslie, A. B., & Callebaut, K. (2001). The petrography of lime inclusions of historic lime based mortars. In M. Stamatacis (Ed.): Proceedings of the 8th Euroseminar on Microscopy applied to building materials. Annales Géologiques des pays Helléniques. Athen, pp. 359–364.

Jackson, M. D., Logan, J. M., Scheetz, B. E., Deocampo, D. M., Cawood, C. G., Logan, J. M., Scheetz, B. E., Deocampo, D. M., Cawood, C. G., Marra, F., Vitti, M., & Ungaro, L. (2009). Assessment of material characteristics of ancient concretes, Grande aula, Markets of Trajan, Rome. *Journal of Archaeological Science*, *36*, 2481–2492. https://doi.org/10.1016/j.jas.2009.07.011

Kitamura, M. (2001). Crystallization and transformation mechanism of calcium carbonate polymorphs and the effect of magnesium ion. *Journal of Colloid and Interface Science*, *236*, 318–327. https://doi.org/10.1006/jcis.2000.7398

Lancaster, L. C. (2021). Mortars and plasters—How mortars were made. The literary sources. *Archaeological and Anthropological Sciences*, *13*, 192. https://doi.org/10.1007/s12520-021-01395-0

Leslie, A. B., & Hughes, J. J. (2002). Binder microstructure in lime mortars: Implications for the interpretation of analysis results. *Quarterly Journal of Engineering Geology and Hydrogeology*, *35*, 257–263. https://doi.org/10.1144/1470-923601-27

Lippmann, F. (1973). *Sedimentary carbonate minerals*. Springer Berlin, Heidelberg. https://doi.org/10.1007/978-3-642-65474-9

Mannoni, T., Pesce, G., & Vecchiattini, R. (2006). Mortiers de chaux dolomitique avec adjonction de kaolin cuit: l'expérience génoise. *ArchéoSciences*, *30*, 67–79. https://doi.org/10.4000/archeosciences.165

Maravelaki-Kalaitzaki, P., Bakolas, A., & Moropoulou, A. (2003). Physico-chemical study of Cretan ancient mortars. *Cement and Concrete Research*, *33*, 651–661. https://doi.org/10.1016/S0008-8846(02)01030-X

Miriello, D., Barca, D., Bloise, A., Ciarallo, A., Crisci, G. M., de Rose, T., Gattuso, C., Gazineo, F., & La Russa, M. F. (2010). Characterisation of archaeological mortars from Pompeii (Campania, Italy) and identification of construction phases by compositional data analysis. *Journal of Archaeological Science*, *37*, 2207–2223. https://doi.org/10.1016/j.jas.2010.03.019

Montana, G., Iliopoulos, I., Tardo, V., & Greco, C. (2009). Petrographic and geochemical characterization of Archaic–Hellenistic tableware production at Solunto, Sicily. *Geoarchaeology: An International Journal*, *24*(1), 86–110. https://doi.org/10.1002/gea.20251

14754754, 0, Downloaded from https://onlinelibrary.wiley.com/doi/10.1111/arcm.12853 by CNR GROUP 11 Istituto di Scienza dell', Wiley Online Library on [16/03/2023]. See the Terms and Conditions (https://onlinelibrary.wiley.com/terms-and-conditions) on Wiley Online Library for rules of use; OA articles are governed by the applicable Creative Commons License

Montana, G., Randazzo, L., Cerniglia, M. R., Aleo Nero, C., & Spatafora, F. (2016). Production technology of early-Hellenistic lime-based mortars originating from a Punic–Roman residential area in Palermo (Sicily). *International Journal of Conservation Science*, *7*(2), 797–812.

Montana, G., Randazzo, L., Vassallo, S., & Udine, F. (2018). The mosaic of the frigidarium of 'villa Bonanno' in Palermo: Mineralogical and petrographic analyses for in situ conservation and restoration interventions. *Mediterranean Archaeology and Archaeometry*, *18*(5), 95–107.

Montana, G., Randazzo, L., Ventura-Bordenca, C., Giarrusso, R., Baldassari, R., & Polito, A. M. (2019). The production cycle of lime-based plasters in the late Roman settlement of Scauri, on the island of Pantelleria, Italy. *Geoarchaeology: An International Journal*, *34*(6), 631–647. https://doi.org/10.1002/gea.21697

Moropoulou, A., Biscontin, G., Bisbikou, K., Theoulakis, P., Theodoraki, A., Tsiourva, Th., & Zendri, E. (1993). Opus caementitium mortars in a polluted and marine atmosphere. In G. Biscontin, D. Mietto (Eds.): Atti del Convegno Scienza e Beni Culturali, 'Calcestruzzi Antichi e Moderni'. Bressanone, 6–9 luglio 1993. Padova (Scienza e beni culturali, 9), pp. 357–371.

Pavía, S., & Caro, S. (2008). An investigation of Roman mortar technology through the petrographic analysis of archaeological material. *Construction and Building Materials*, *22*, 1807–1811. https://doi.org/10.1016/j.conbuildmat.2007.05.003

Pavía, S., Fitzgerald, B., & Howard, R. (2005). Evaluation of properties of magnesian lime mortar. In C. A. Brebbia, A. Torpiano (Eds.): Structural Studies, Repairs and Maintenance of Heritage Architecture IX. Transaction on the built environment: WIT Press (83), pp. 375–384.

Pecchioni, E., Fratini, F., & Cantisani, E. (2020). *Atlas of the ancient mortars in thin section under optical microscope* (2nd ed.). Nardini.

Portale, C. E. (2006). Problemi dell'Archeologia della sicilia ellenistico-romano: Il caso di Solunto. *Archaeologica Classica*, *57*, 49–114.

Pouchou, J. L., & Pichoir, F. (1991). *Quantitative Analysis of Homogeneous or Stratified Microvolumes Applying the Model "PAP"*. In Electron Probe Quantitation; Springer: Boston, MA, USA, pp. 31–75.

Ricca, M., Galli, G., Ruffolo, S. A., Sacco, A., Aquino, M., & La Russa, M. F. (2019). An archaeometric approach of historical mortars taken from Foligno City (Umbria, Italy): New insight of Roman empire in Italy. *Archaeological and Anthropological Sciences*, *11*, 2649–2657. https://doi.org/10.1007/s12520-018-0706-7

Schmölder-Veit, A., Henke, F., Thiemann, L., Schlütter, F., & Jackson, M. D. (2016). Hydraulische Mörtel. Interdisziplinäres Projekt zu Wasseranlagen auf dem Palatin. *Römische Mitteilungen*, *122*, 331–366.

Schön, F. (2015). '… auf dass ihnen das Wasser nicht ausgeht'- Antike Kleinwasserspeicher im Zentralen und westlichen Mittelmeerraum (2) (unpl.).

Schön, F., Amicone, S., Berthold, C., Boese, B., & König, T. P. (2019). Archaeometric Data for the Urbanistic Development of Solunto (Sicily/Italy)—The Casa di Arpocrate. First Results of the Tuebingen Mortar Project. In M. Trümper, G. Adornato, T. Lappi (Eds.): Cityscapes of Hellenistic Sicily. Proceedings of a Conference of the Execellent Cluster Topoi. The Formation and Transformation of Space and Knowledge in Ancient Civilization, 15.–18. June 2017. Rome, pp. 113–128.

Schork, J. (2012). Dolomitic lime in the US. History, development and physical characteristics. *Journal of Architectural Conservation*, *18*(3), 7–25. https://doi.org/10.1080/13556207.2012.10785116

Sposito, A. (2014). *Solunto*. Paesaggio Città Architettura.

Toffolo, M. B. (2020). Radiocarbon Dation of anthropogenic carbonates: What is the benchmark for sample selection. *Heritage*, *3*, 1416–1432. https://doi.org/10.3390/heritage3040079

Tusa, V. (1994). Storia degli scavi e degli studi. In A. Cutroni Tusa, A. Italia, D. Lima, & V. Tusa (Eds.), *Solunto* (pp. 12–16). Istituto Poligrafico e Zecca dello Stato, Libreria dello Stato.

Weber, J., Prochaska, W., & Zimmermann, N. (2009). Microscopic techniques to study Roman renders and mural paintings from various sites. *Materials Characterization*, *60*(7), 586–593. https://doi.org/10.1016/j.matchar.2008.12.008

Whitney, D. L., & Evans, B. W. (2010). Abbreviations for names of rock-forming minerals. In. *American Mineralogist*, *95*, 185–187. https://doi.org/10.2138/am.2010.3371

Wolf, M. (2003). *Die Häuser von Solunt und die Hellenistische Wohnarchitektur. Sonderschriften des DAI Roms 14*. P. von Zabern (Mainz).

SUPPORTING INFORMATION

Additional supporting information can be found online in the Supporting Information section at the end of this article.

How to cite this article: Boese, B., Amicone, S., Cantisani, E., Schön, F., & Berthold, C. (2023). Mortars in context: An integrated study of mortars and plasters from the so-called *Ginnasio* in Solunto (Sicily, Italy). *Archaeometry*, 1–19. https://doi.org/10.1111/arcm.12853

14754754, 0, Downloaded from https://onlinelibrary.wiley.com/doi/10.1111/arcm.12853 by CNR GROUP 11 Istituto di Scienza dell', Wiley Online Library on [16/03/2023]. See the Terms and Conditions (https://onlinelibrary.wiley.com/terms-and-conditions) on Wiley Online Library for rules of use; OA articles are governed by the applicable Creative Commons License